

# Multifunctional materials for clean energy conversion

R. Krishnapriya<sup>1</sup>, Devika Laishram<sup>1</sup>, M. Shidhin<sup>2</sup>, Rakesh K. Sharma<sup>1</sup>

<sup>1</sup>Sustainable Materials and Catalysis Research Laboratory, Department of Chemistry, Indian Institute of Technology Jodhpur, Jodhpur, Rajasthan, India

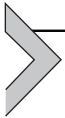
<sup>2</sup>The Department of Metallurgical and Materials Engineering, Indian Institute of Technology, Chennai, Tamil Nadu, India

## 4.1 Introduction

With the rapid depletion of fossil fuels, rising environmental concerns, and population growth, it is inevitable to develop clean energy technologies to power our future society [1–4]. These energy conversion and storage technologies are anticipated to be sustainable and also capable of meeting our long-term energy needs. During the past few years, extensive research interests have been devoted to the advancement of energy conversion devices, as they play a crucial role in the prosperity and economic growth of a country. Particularly, the energy conversion technologies such as solar and fuel cells have proved to be highly reliable and can offer clean and sustainable energy at affordable rate [5–8]. However, the performance potential of these devices, such as output voltage, conversion efficiency, and stability, are greatly relied on the materials used. The energy conversion process comprises physical and/or chemical reactions at the surface of the material or at its interfaces; hence, the specific surface area, surface energy, and even surface chemistry can critically affect the device performance.

Recently, the use of nanomaterials as the building blocks to fabricate energy conversion devices has opened up a novel path for the development of highly efficient and robust electrode materials with required properties [9,10]. These materials exhibit exceptional electrical conductivity, thermal conductivity, dielectric constant, and mechanical quality factor owing to the quantum dimension effects and macroscopic quantum tunneling effects. The lower dimensions of nanomaterials offer satisfactory mass, heat, and charge transfer through the advantage of accommodation of dimensional variations in accordance with chemical reactions and phase transitions. Among different nanomaterials, multifunctional nanomaterials are receiving

specific attention. These materials can show distinct optical, magnetic, and electrical properties, which are anticipated to offer enhanced performance when applied in a device [11,12]. Generally, the materials that are designed to perform multiple roles via a prudent combination of several functions are called multifunctional materials. The research on these materials involves understanding the structure–property relationship that is leading to the design and fabrication. However, the fabrication of multifunctional material with desirable functions is relatively challenging, from searching for novel materials, understanding its properties, and tuning the properties in order to apply in a technological device. In this chapter, a comprehensive summary of various multifunctional nanomaterials at a broader perspective to overcome the challenges of energy conversion devices is presented.



## **4.2 Energy conversion devices**

### **4.2.1 Solar cells**

There are different energy conversion devices that effectively use the nanostructured materials to convert the energy into a useful form. Among these, solar cells are the central energy conversion devices that deliver clean electrical energy, where the renewable solar energy is directly converted into electrical energy without releasing any greenhouse gases. The main features of solar cells are the internal and external quantum efficiency and energy conversion efficiency. Solar cells are mainly classified into three types. The first-generation silicon solar cells made of Si wafers and mainly single crystal-based on p–n junctions, which are the most widely used solar cells and which have taken over the current photovoltaic (PV) device market and have reported maximum efficiency of nearly 25% [13]. The second-generation PV devices use thin-film technologies, which include cadmium telluride (CdTe), copper indium gallium diselenide (CIGS), and amorphous thin-film silicon. However, the efficiency is much below that of silicon solar cells. Third-generation solar cells include solution processing technology of semiconducting organic macromolecules, inorganic nanoparticles, or hybrids [14]. Copper zinc tin sulfide solar cell, dye-sensitized solar cells (DSSC), organic solar cells, perovskite solar cells, and quantum dot solar cells (QDSC) come under this classification. A schematic representation of the different generations of solar cells and their achieved efficiencies are given in Fig. 4.1.

Among different types of solar cells such as DSSCs, hybrid organic solar cells and QDSCs are based on the advances in nanotechnology [15–18].

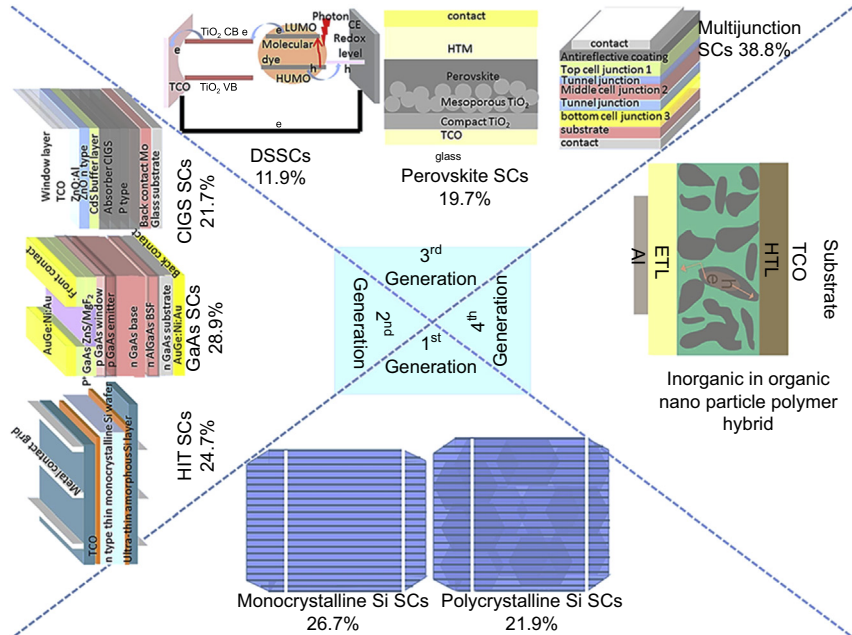


**Figure 4.1** Schematic diagram showing the evolution of different generations of photovoltaic solar cells with respective device structures and the current photovoltaic efficiencies. Reproduced with permission from Elsevier A. Sahu, A. Garg, A. Dixit, *A review on quantum dot sensitized solar cells: past, present and future towards carrier multiplication with a possibility for higher efficiency*, *Sol. Energy* 203 (2020) 210–239.

The solar energy harvesting and its conversion is achieved by nanostructured semiconductor interface with a dye in case of DSSC, a conjugate polymer in organic solar cells, and semiconductor nanocrystals for QDSCs [19]. Improving the efficiency of these devices involve bringing the effective photo-induced charge separation, as well as the transport of charge carriers across the nanoassemblies, which is the main challenge. The advance of nanoassemblies to improve light harvesting efficiency, thermodynamic and kinetic measures for effective device design, and approaches for effective utilization of photo-induced charge separation in donor-acceptor molecules to fabricate nanostructure-based solar cells are the hot topic of research in recent years [2,20–22].

## 4.2.2 Fuel cells

Fuel cells are energy conversion devices that can convert chemical energy from a fuel into electrical energy via a reaction with oxygen or other

oxidizing agents. Recently, fuel cells are getting considerable consideration as an alternative energy source owing to their high efficiency without the release of harmful chemicals to the surroundings. The basic structure of a fuel cell contains an electrolyte that is in contact with a porous anode and a cathode. The fuel comes into the anode, and then an oxidant moves in through cathode, which is divided by a selectively conductive electrolyte. Further, the conduction occurs through the electrolyte in either anode to cathode or cathode to anode direction. The main conductive charge carriers comprise  $H^+$ ,  $CO_3^{2-}$ ,  $O^{2-}$ ,  $OH^-$ , etc. [23,24]. The important commercial fuel cell technologies are divided into many groups in accordance with the operating conditions and which is given in Fig. 4.2.

The most efficient and widely used fuel cells applied in cellular phones and laptops are direct methanol fuel cells and proton exchange membrane fuel cells because of their high power density and lower operating temperatures [25–28]. However, there are some challenges faced by fuel cell technology, such as fabricating suitable electrodes for the flexible electronics, replacing the high-cost noble metal electrocatalysts, and preventing electrode poisoning. The major challenge associated with this technology is the cost of fuel. However, significant advances in the development of materials with improved properties can make this technology more reliable. Current research is focused on the development of high-efficiency fuel cells of low cost with ecofriendly nanostructured electrode materials [29,30].

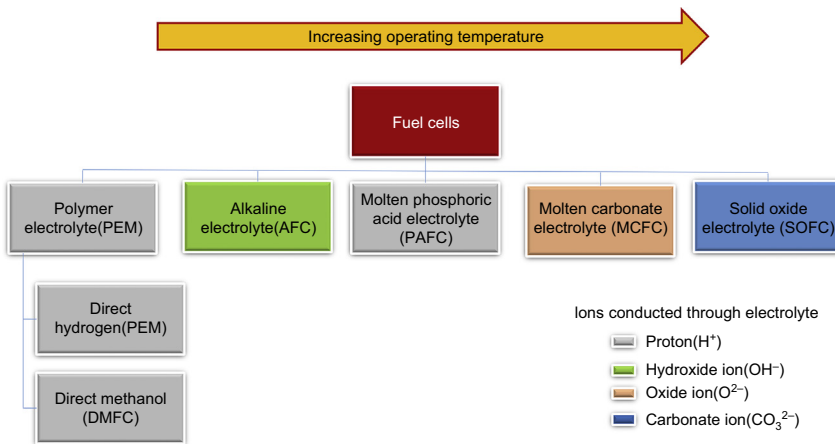
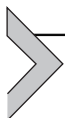


**Figure 4.2** Types of different commercially available fuel cells.



### 4.3 Multifunctional nanomaterials for energy conversion applications

The primary requirement of nanostructured materials for PV devices such as DSSCs and QDSCs is to have a large specific surface area for the anode to adsorb sufficient dye molecules and quantum dots (QDs). This can act as an antenna for light absorption. To achieve the maximum absorption of incident light, the narrow thickness of photoanode with minimum interface charge recombination is desired [31–33]. Moreover, the material must possess remarkable charge mobility and long lifetime, with some light scattering effect or photon trapping ability.

Fuel cell technology faces significant challenges like low energy density, power density, and operation reliability along with the high cost. Nanostructured materials can overcome most of these challenges by providing high specific surface area and improved conductivity with low polarization. These materials have the potential to offer excellent nanoporous structures with multifunctional chemical properties for highly intrinsic electroactivity and excellent utilization [34].

Nanostructured semiconductor metal oxides of  $\text{TiO}_2$ ,  $\text{ZnO}$ ,  $\text{SnO}_2$ ,  $\text{Fe}_2\text{O}_3$ ,  $\text{WO}_3$ , and  $\text{BiVO}_4$  were extensively explored as photoelectrode materials for solar cells owing to their tunable semiconducting properties, high stability, and easy fabrication. Mesoscopic  $\text{TiO}_2$  film is the main component of DSSCs, organic photovoltaics, and QDSCs, which helps to capture electrons from the excited sensitizer or quantum dot and allows the easy transport of electrons to the transparent collecting electrode [35,36]. The charge separation and transports occur at the photoelectrode/electrolyte interface or within the photoelectrode which is critical for device performance. These reactions mainly depend on the morphology and structure of metal oxide used. Thus, metal oxides of different morphologies have been applied to tailor optical and electronic properties. A systematic study on the influence of hierarchically structured morphology of different metal oxide (MO) photoanodes on the performance of DSSCs was reported by various research groups [37–39]. Sun and coworkers reported a novel multifunctional photoanode consisting of one-dimensional (1D)  $\text{TiO}_2$  nanotube arrays modified by  $\text{TiO}_2$  nanoparticles as the bottom layer and three-dimensional (3D)  $\text{TiO}_2$  submicron spheres as the top layer by a facile one-pot chemical bath deposition method. The prepared 1D–3D bilayer photoanode demonstrates a power conversion efficiency (PCE) of 6.93%, leading to a 26.5% increment of PCE compared to 5.48% by  $\text{TiO}_2$  bare nanotube arrays [40]. A high PCE of

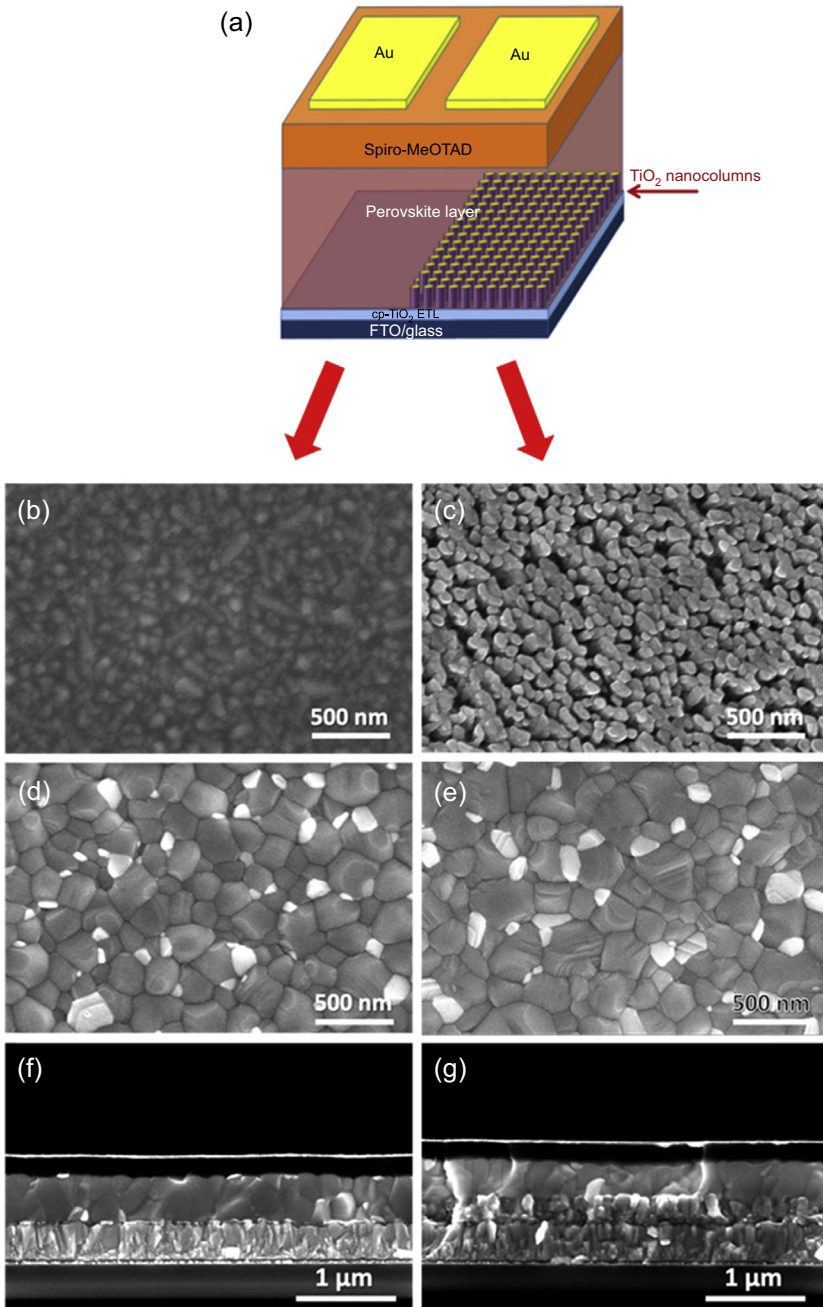


**Figure 4.3** (a) Schematics of the perovskite solar cell architecture with half of its interface covered by cp-TiO<sub>2</sub> ETL and the other half covered by TiO<sub>2</sub> nanocolumn arrays.

9.3% was reported by single crystallike anatase  $\text{TiO}_2$  nanowires network prepared by an “oriented attachment” mechanism. The resulting nanowire (NW) shows the high rate of electron transfer through the  $\text{TiO}_2$  film [41]. The effect of length of nanotube can also influence the PCE of DSSC which was reported by Liu et al. Nanotubes (NTs) with length up to 20.8  $\mu\text{m}$  were achieved which improved the PCE [42]. Recently, vertically aligned 1D  $\text{TiO}_2$  nanocolumn arrays were fabricated by glancing angle deposition to apply as electron transport layer (ETL) to fabricate functional triple-cation lead perovskite halide solar cells based on  $\text{Cs}_{0.05}(\text{FA}_{0.83}\text{MA}_{0.17})_{0.95}\text{Pb}(\text{I}_{0.83}\text{Br}_{0.17})_3$  [43]. The schematic representation of the device architecture and the scanning electron microscopy (SEM) images of  $\text{TiO}_2$  nanocolumn are given in Fig. 4.3.

A promising PCE of 16.38% with 5% boost of short-circuit current density and a 7% improvement in its power conversion efficiency, together with a significantly prolonged shelf life, were obtained by careful tuning of the  $\text{TiO}_2$  column properties. Another potential MO for DSSCs are  $\text{ZnO}$  and  $\text{SnO}_2$ ; they have a energy band position and physical properties comparable to  $\text{TiO}_2$  but these materials have higher electron mobility, which is capable of improving the electron transport efficiency leading to reduction in recombination loss. Morphology engineering of  $\text{ZnO}$ , doping, heterostructures of  $\text{ZnO}/\text{TiO}_2$ , phase and dimensionally controlled synthesis of oxides at subzero temperatures, etc., succeeded in improving the efficiency of solar cells [44–49]. The  $\text{ZnO}$  morphology-dependent PCEs of DSSCs with respect to various reaction conditions are given in Fig. 4.4.

$\text{ZnO}$  demonstrated as a promising ETL to  $\text{TiO}_2$  for perovskite solar cells (PSCs) exhibiting remarkable efficiency of 18.9% [50]. Recently,  $\text{ZnO}$  with a high crystallization multiple cation perovskite absorber showed a high efficiency of over 20% [51]. Compared to  $\text{TiO}_2$  photoanodes,  $\text{SnO}_2$ -based DSSCs are showing less PCE. Zhang et al. fabricated  $\text{SnO}_2@\text{Air}@\text{TiO}_2$  hierarchical urchinlike double-hollow nanospheres as

(b, c) Top-view SEM images of the cp- $\text{TiO}_2$  layer (b) and the  $\text{TiO}_2$  nanocolumn arrays (c). (d, e) SEM image of the perovskite film deposited on a cp- $\text{TiO}_2$  ETL (d) and on  $\text{TiO}_2$  nanocolumn arrays (e). (f, g) Cross-sectional SEM image after the deposition of a hole transport polymer on the part of the sample with only a cp- $\text{TiO}_2$  ETL (without nanocolumns, (f) and the part of the sample with  $\text{TiO}_2$  nanocolumn arrays (g). *Reproduced with permission from American Chemical Society Z. Hu, J.M. García-Martín, Y. Li, L. Billot, B. Sun, F. Fresno, A. García-Martín, M.U. González, L. Aigouy, Z. Chen,  $\text{TiO}_2$  nanocolumn arrays for more efficient and stable perovskite solar cells, ACS Appl. Mater. Interfaces 12 (5) (2020) 5979–5989.*

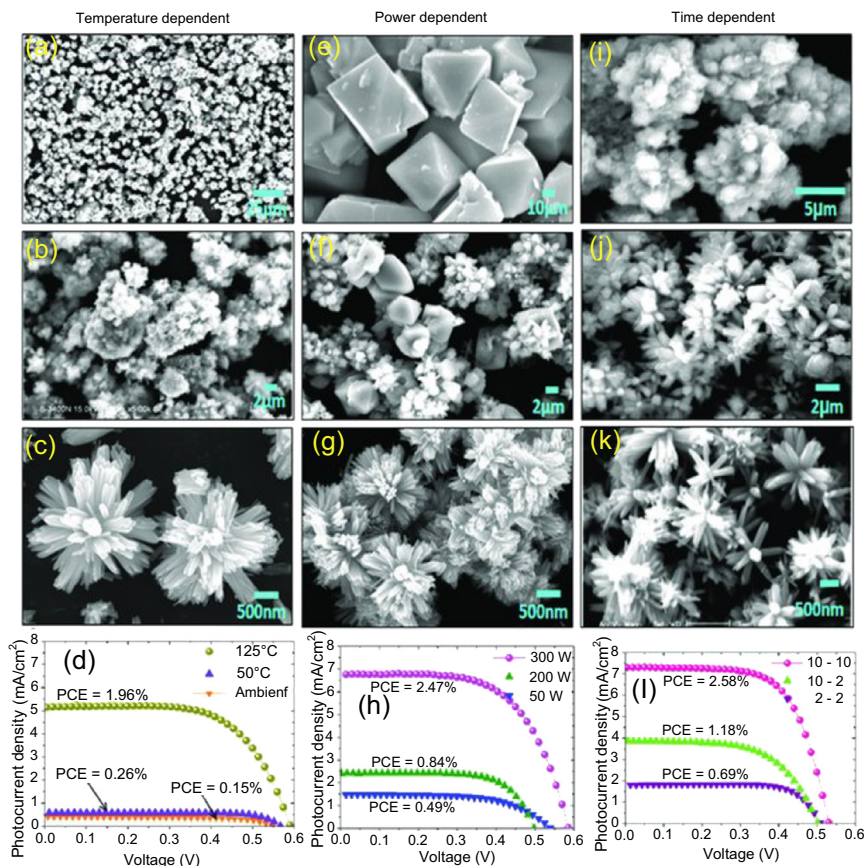


**Figure 4.4** A comparative study of morphology-dependent J-V curves of hierarchical ZnO flower growth stages illustrated in FE-SEM images. *Reproduced with permission from Royal Society of Chemistry R. Krishnapriya, S. Praneetha, A.V. Murugan, Investigation of the effect of reaction parameters on the microwave-assisted hydrothermal synthesis of hierarchical jasmine-flower-like ZnO nanostructures for dye-sensitized solar cells, New J. Chem. 40 (6) (2016) 5080–5089.*

photoanode. This composite structure of DSSC demonstrated a maximum efficiency of 6.77% owing to the increased transmission of photogenerated electrons [52]. Composite and hybrid photoanodes are another promising alternative for improved performance of DSSCs. GO/SnO<sub>2</sub> hybrid nanocomposite-based photoanode for DSSCs have achieved a PCE of 8.3% with higher dye-loading, rapid electron transport, superior light scattering, and lower electron recombination rate [53]. Doping of lithium ions is proved to be the best way to improve the PCE of SnO<sub>2</sub>-based solar cells.

Park et al. reported the fabrication of a highly stable and efficient electron transporting layer using Li-doped  $\text{SnO}_2$  ( $\text{Li}:\text{SnO}_2$ ) relatively at low temperature in wet-chemical route [54]. The doped Li in  $\text{SnO}_2$  improved conductivity and favored a downward shift of the conduction band minimum of the oxide, which enabled easy path for the electrons injection and transfer from conduction band of perovskite. An exceptionally high PCE of 18.2% and 14.78% were achieved for the rigid and flexible substrates, respectively, which is shown in Fig. 4.5.

Perovskites are naturally occurring minerals of  $\text{CaTiO}_3$ , and the materials which have same type of crystal structure as  $\text{CaTiO}_3$  are generally called perovskite materials [55]. These materials possess a cubic or tetragonal crystal structure with the stoichiometric formula  $\text{AMX}_3$ , where both A and M are metal cations with A larger than B and X is the anion, usually oxides or halogens [56]. Commonly, each cation M is octahedrally coordinated with the anion X to form  $\text{MX}_6$  octahedra (Oh), which is the basic building block of the perovskite structure. These Oh units are connected in a 3D corner-sharing configuration, with the cation A surrounded in the space formed between adjacent  $\text{MX}_6$  octahedron to neutralize the charge of the structure. The unique physical properties of perovskite materials such as high-absorption coefficient, long-range ambipolar charge transport, low exciton binding energy, high dielectric constant, ferroelectric properties, etc., make this material a suitable candidate for photovoltaic applications. Distortions exist in the perovskite structure that results in oxygen nonstoichiometry comprising both oxygen deficiency and oxygen excess. Thus, perovskite oxides offer great flexibility in redox active sites, oxygen vacancies, and physicochemical properties with tunable compositions due to the numerous possible substitutions at both A and B sites. Perovskite oxides can exist in different structures such as double perovskites and layered perovskite. Owing to its varied compositions and structure, the material offers excellent thermal stability, redox properties, oxygen mobility, and electronic and ionic conductivity; perovskites became very attractive in solar cells around the world. With the advantage of unprecedentedly superb optoelectronic properties, together with a carrier diffusion length of up to  $\sim 100 \mu\text{m}$  and a low exciton binding energy of  $\sim 20 \text{ meV}$ , this material enables the formation of free carriers even at room temperature, high optical absorption coefficient of  $\sim 10^5 \text{ cm}^{-1}$ , and low nonradiative recombination for optoelectronic device applications. PSCs have shown more impressive progress than other PV technology with the certified efficiency of 25.2%. However, the poor stability of the perovskite

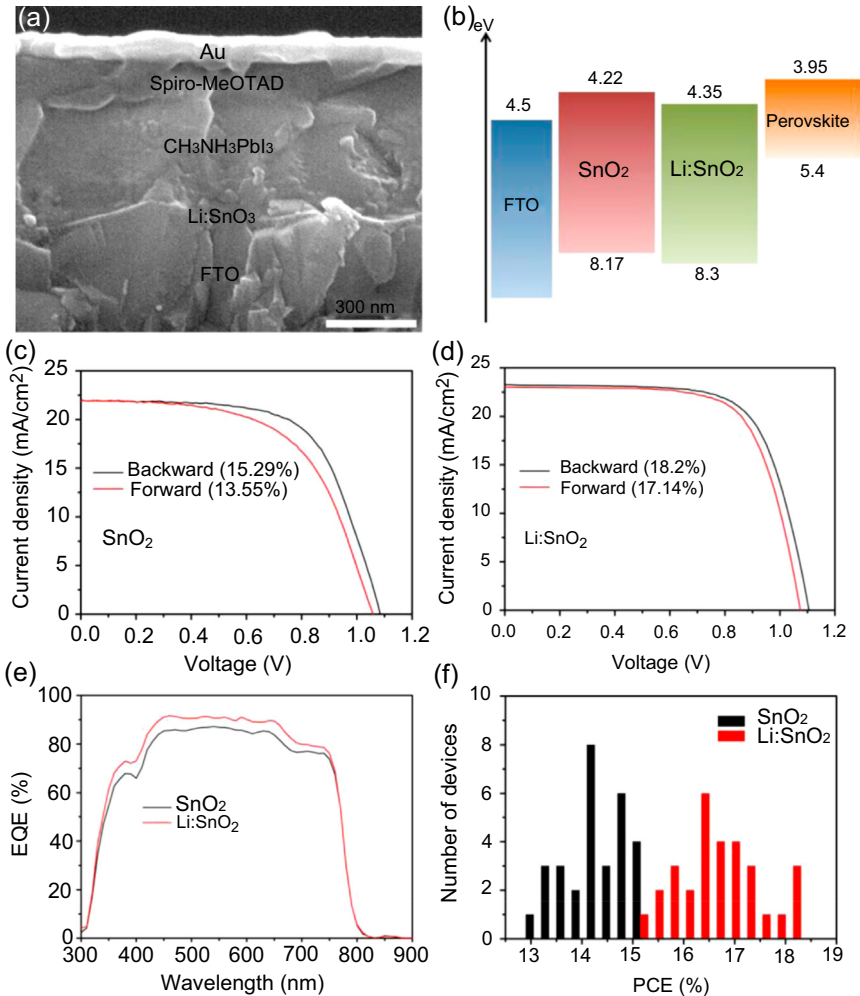


**Figure 4.5** (a) Cross-sectional SEM image of a PSC. (b) Energy diagram of FTO, ETLs, and perovskite ( $\text{CH}_3\text{NH}_3\text{PbI}_3$ ). (c, d) J-V curves measured at backward-forward scan for 200 ms of scan-delay time. The measurements were performed under simulated AM 1.5 G sunlight of  $100 \text{ mW}/\text{cm}^2$ . (e) EQE spectra of the devices comprising  $\text{SnO}_2$  and  $\text{Li:SnO}_2$  as an ETL, respectively. (f) Histogram of PCEs for 30 devices. *Reproduced with permission from M. Park, J.Y. Kim, H.J. Son, C.H. Lee, S.S. Jang, M.J. Ko, Low-temperature solution-processed Li-doped  $\text{SnO}_2$  as an effective electron transporting layer for high-performance flexible and wearable perovskite solar cells, Nano Energy 26 (2016) 208–215.*

materials with regard to humidity, heat, light, and oxygen is the main challenge that should be addressed before its commercialization. Recently,  $\text{CsYbI}_3$  cubic NCs presented strong excitation-independent emission and high photoluminescence quantum yields of 58% [57].

$[\text{HC}(\text{NH}_2)_2]_{0.83}\text{Cs}_{0.17}\text{Pb}(\text{I}_{0.6}\text{Br}_{0.4})_3$ ,  $\text{Cs}^+$ -Doped 2D  $(\text{BA})_2(\text{MA})_3\text{Pb}_4\text{I}_{13}$ , halide perovskites, with a typical structure of  $\text{ABX}_3$  ( $\text{A} = \text{CH}_3\text{NH}_3^+$ ,  $\text{CH}(\text{NH}_2)_2^+$ ,  $\text{Cs}^+$ ; B their achieved efficiencies =  $\text{Pb}^{2+}$ ,  $\text{Sn}^{2+}$ ;  $\text{X} = \text{Cl}^-$ ,  $\text{Br}^-$ ,  $\text{I}^-$ ), and  $\alpha$ - $\text{CsPbI}_3$ -based PSCs showed promising PCE [58,59]. Additionally, perovskite oxides with high ionic/electronic conductivity find good application as anode, cathode, and electrolyte in solid oxide fuel cells (SOFCs) [60,61]. This material is the practical choice at operation at 700–900°C because of high electrochemical activity for the  $\text{O}_2$  reduction reaction, high thermal stability, and compatibility. It shows excellent microstructural stability and long-term performance stability. Perovskite oxides with nanoporous nature exhibited greater powder density and lower area-specific polarization for fuel cell applications [62].

Novel nanostructured carbon-based metal-free electrode materials can be used as superior catalyst supports for energy conversion devices due to their remarkable electric conductivity. These materials can act as efficient photo-/electrocatalysts to enable the crucial chemical reactions. These specific reactions include the oxygen reduction reaction (ORR) in fuel cells and the iodine reduction reaction in DSSCs. The incorporation of p-block elements such as N, P, Si, and B, as well as the heteroatoms (O, S, Se, F, Cl, Br) can greatly improve the device performance. A 3D honey N-doped graphene of the special hierarchical framework structure, high specific surface, and rich N species is used for ORR and OER catalysis. The performance was found to be comparable to the commercial  $\text{RuO}_2$  and Pt [63]. The peculiarity of carbon structures is the intrinsic defects existing in carbon structures, which can induce charge transfer and density of state change, thus creating more active centers for reactions. Various nanoarchitectures, with a range of sizes, shapes, compositions, and structures, have shown good potential to catalyze the reactions in solar cells and fuel cells. Several carbon-based nanostructures, such as fullerenes, nanotubes, and graphene are used in solar cells [64,65]. Graphene is most commonly used for fabrication in carbon-based organic photovoltaic cells due to its excellent electron transport properties and extremely high carrier-mobility. In addition, its energy level can be tuned easily through controlling its size, layers, and functionalization. These materials can be used for the fabrication of transparent conducting electrodes, as composite for semiconducting layer,

in electrolyte and as counter-electrodes. These materials are established as efficient candidates to replace or modify the existing components in solar cells [66]. Carbon nanotube-based PSCs can exhibit higher high-temperature operational stability than those of metal-based electrodes. Interesting report on ex-situ vapor-assisted doping of CNT electrode for efficient and stable PSCs is shown in Fig. 4.6.

The enhanced conductivity with a favorable energy alignment of modified CNT is able to achieve a PCE of 17.56% with greater stability. As the method employed was facile, rapid, and readily applicable to large area, module process can successfully offer a solution to overcome the efficiency limit in CNT-laminated PSCs [67].

In the photoanode, graphene materials have resulted in improved photocurrent. Additionally, an atomically dispersed Co-doped carbon catalyst with a core-shell structure was developed via a surfactant-assisted metal-organic framework approach and applied to fuel cells. The  $\text{CoN}_4$  active sites in catalysts revealed unprecedented catalytic activity for ORR with a half-wave potential of 0.84 V and promising stability in challenging acidic media [68]. N-Doped carbon nanobubbles, spheres, and their graphene composites have also showed long-term operational stabilities and comparable gravimetric power densities when applied in various energy device applications [69,70].

Owing to the advantages like low cost, earth abundance, and ease of synthesis and practical applications, metal chalcogenides (MC) have found great importance for application in energy conversion devices. These nanostructured materials have found to be an effective alternative to Pt/C electrocatalysts in fuel cells. Baresel *et al.* reported the electrocatalytic activity of thiospinels and other sulfides for oxygen reduction in acidic electrolytes [71]. Later, chevrel-phase  $\text{Mo}_4\text{Ru}_2\text{Se}_8$  chalcogenides and related compounds were reported and showed interesting catalysis properties [72]. Various MC of cobalt, nickel, and iron show unique electrical properties, excellent catalytic activities, and outstanding stabilities. These materials were successively used as counter-electrodes (CE) for DSSCs. Electrochemically deposited CoS NPs on flexible conducting oxide films have reported 6.5% of PCE [73]. Accordingly, sulfides and selenides of iron, cobalt, and nickel ( $\text{FeS}_2$ ,  $\text{FeSe}$ ,  $\text{Co}_{0.85}\text{Se}$ , and  $\text{NiSe-Ni}_3\text{Se}_2$ ) have been reported extensively as potential low-cost CE materials [74–76]. Chang *et al.* prepared

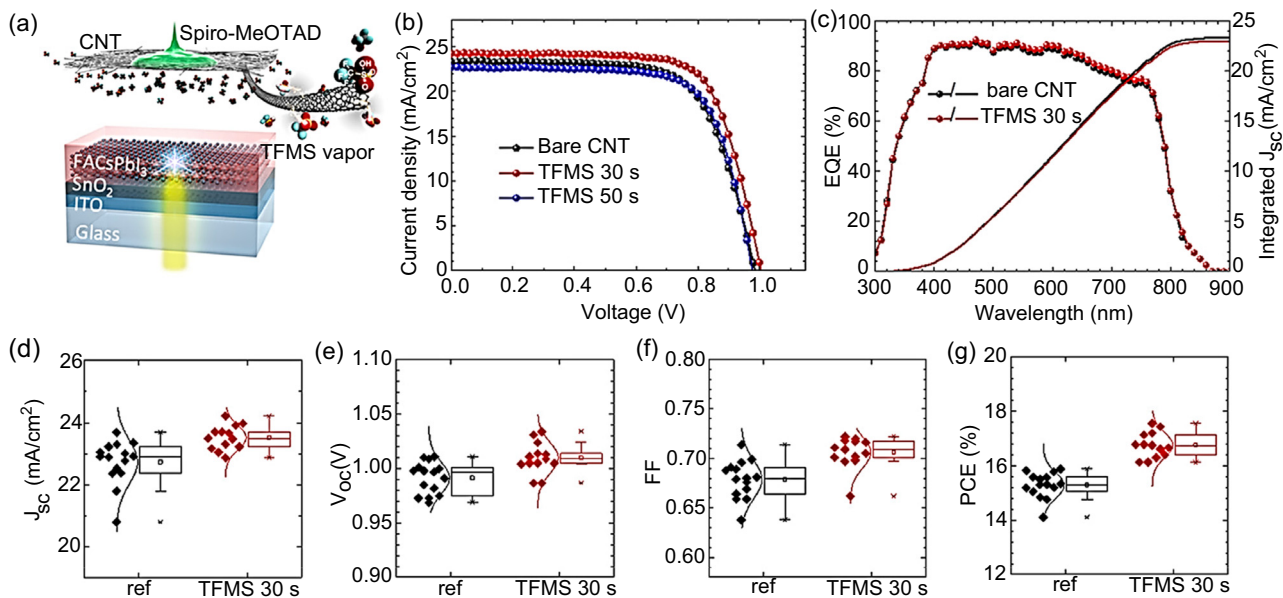


**Figure 4.6** (a) Schematic illustration showing structure of planar heterojunction perovskite solar cells based on TFMS doped CNT (b) Current density-voltage ( $J$ - $V$ ) curves of the highest efficiency perovskite solar cells incorporating bare CNT and CNT doped by TFMS (30 and 50 s of doping time). (c) EQE spectra and corresponding integrated short-circuit current density ( $J_{sc}$ ) of the device based on bare CNT and CNT doped by TFMS for 30 s (d)  $J_{sc}$ , (e) open circuit voltage ( $V_{oc}$ ), (f) fill factor (FF) and (g) power conversion efficiency (PCE) of the perovskite solar cells incorporating bare CNT and CNT doped by TFMS. *Reproduced with permission from American Chemical Society J.W. Lee, I. Jeon, H.S. Lin, S. Seo, T.H. Han, A. Anisimov, E.I. Kauppinen, Y. Matsuo, S. Maruyama, Y. Yang, Vapor-assisted ex-situ doping of carbon nanotube toward efficient and stable perovskite solar cells, Nano Lett. 19 (4) (2019) 2223–2230.*

$\text{Co}_9\text{S}_8$  nanocrystal-based nanoinks to fabricate uniform, crack-free  $\text{Co}_9\text{S}_8$  thin films with a spray deposition technique, and when applied as counter electrode (CE) for DSSC showed PCE of  $7.02 \pm 0.18\%$  under AM 1.5 solar illumination [77]. The morphological features and the photoelectrical and electrochemical characteristics of the synthesized material are shown in Fig. 4.7.

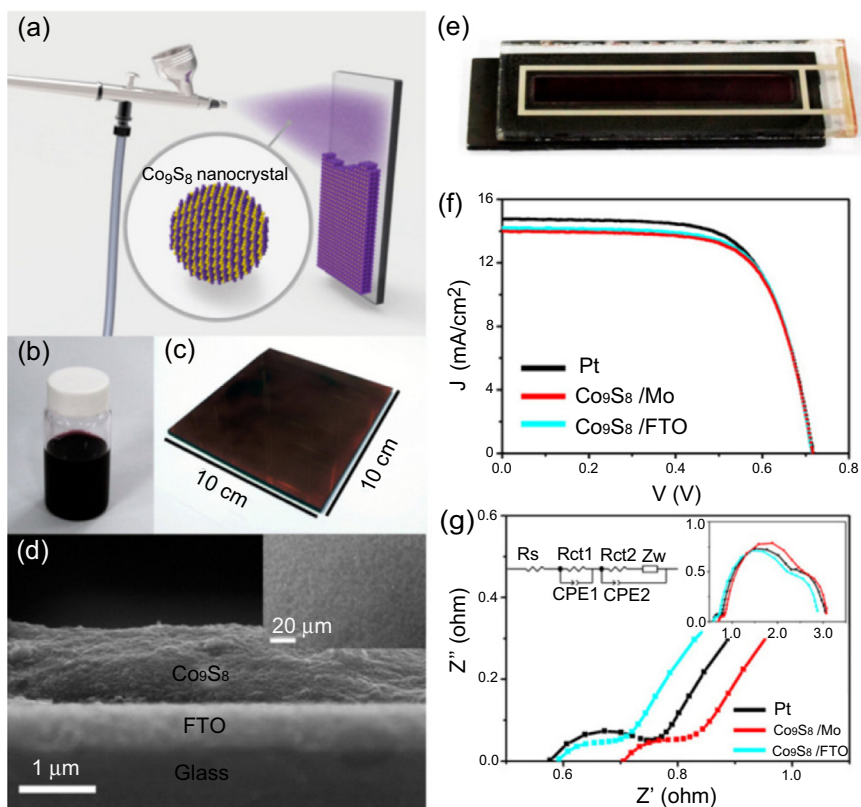


**Figure 4.7** (a) Schematic diagram of  $\text{Co}_9\text{S}_8$  nanocrystals synthesized on FTO by spray deposition; (b) Photograph of  $\text{Co}_9\text{S}_8$  nanoink for the thin-film deposition; (c) Photograph of the  $\text{Co}_9\text{S}_8$  nanocrystal thin film deposited on a  $10 \text{ cm} \times 10 \text{ cm}$  FTO substrate; (d) SEM image of the cross-sectional and plan (inset) views of the  $\text{Co}_9\text{S}_8$  film/FTO; (e) Photograph of a simulated DSSC cell with  $2 \text{ cm}^2$  working area; (f) Photocurrent density-voltage plots of DSSCs based on platinum,  $\text{Co}_9\text{S}_8$  on FTO, and  $\text{Co}_9\text{S}_8$  on Mo CEs obtained under AM1.5 illumination; (g) Nyquist curves of the DSSCs based on platinum,  $\text{Co}_9\text{S}_8$  on FTO, and  $\text{Co}_9\text{S}_8$  on Mo CEs. *Reproduced with permission from American Chemical Society.*

Moreover, along with monometallic chalcogenides, binary and ternary MC have been successfully applied as CE materials for DSSCs because of their exceptional electrochemical properties. By the careful control over chemical composition, ternary and polyphyletic compounds based on iron, cobalt, and nickel, such as NiCoSe, Co-Fe-Se/S, and NiCo<sub>2</sub>O<sub>4</sub>, provided catalytically active CE with good electronic conductivity [78–80]. Bimetal transition metal alloys and compounds such as MIn<sub>2</sub>S<sub>4</sub> (M = Fe, Co, Ni), NiCo<sub>2</sub>S<sub>4</sub>, CoFeS<sub>2</sub>, and (Ni, Fe) S<sub>2</sub> also successfully reported and exhibited high performances due to the coexistence of two different cations in a single crystal structure [81,82]. Among them, siegenite (NiCo<sub>2</sub>S<sub>4</sub>) with a normal thiospinel crystal structure unveils outstanding electrocatalytic performance due to the synergistic interactions between Co<sup>2+/3+</sup> and Ni<sup>2+</sup>. The hierarchical nanostructured NiCo<sub>2</sub>S<sub>4</sub> with urchinlike, porous sheetlike, hexagonal, and flowerlike morphologies has been extensively reported for Pt-free DSSCs. However, the use of pristine materials as CEs is facing metal aggregation problems; so its application in DSSCs is limited. A possible solution to this problem is to make a composite with graphene. Graphene is particularly interesting because of its layers of two-dimensional (2D) sp<sup>2</sup>-bonded carbon sheets, its unique structure, and exceptional physical properties, such as high electrical and thermal conductivities, mechanical flexibility, charge transport mobility, huge specific surface area, good chemical stability, and optical transparency. Thus, nanocomposites of carbon nanotube and graphene-integrated transition metal-based electrocatalysts have abundant research consideration. Accordingly, the growth of nanocrystalline NiCo<sub>2</sub>S<sub>4</sub> on graphene nanosheets (GNSs) has been reported as the GNSs serve as 2D electrical conductive scaffold to electroactive NiCo<sub>2</sub>S<sub>4</sub> and also are capable of enhancing charge transport factors, thereby refining the electrochemical performance. A sustainable rapid microwave-solvothermal (MW-ST) synthesis approach to develop NiCo<sub>2</sub>S<sub>4</sub> nanocrystals and their nanohybrids with GNS was reported with a PCE of 7.98% [83]. The morphological features and the PV performance of the CE are given in Fig. 4.8.

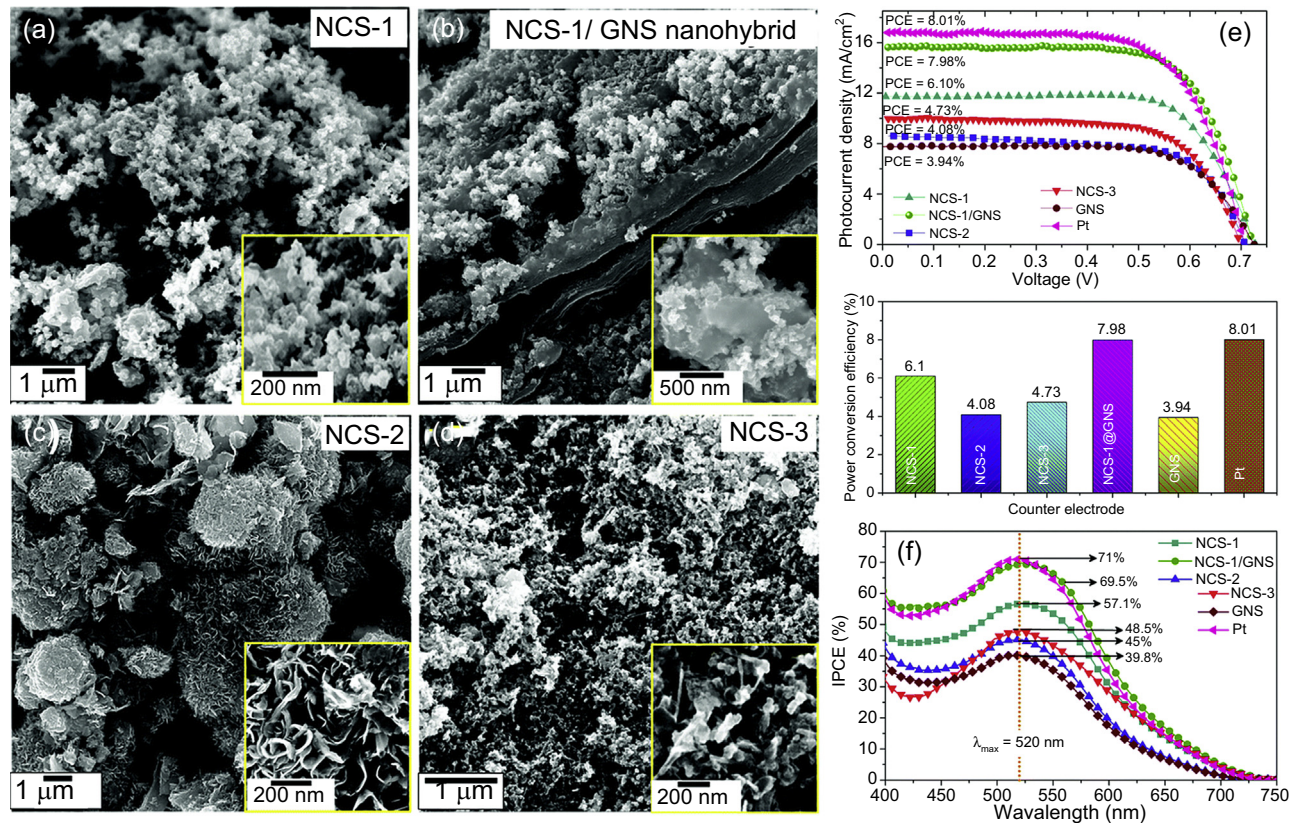
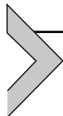


**Figure 4.8** FE-SEM images of NiCo<sub>2</sub>S<sub>4</sub> nanocrystals with (a) nanocrystalline aggregates (NCS-1), (b) the NiCo<sub>2</sub>S<sub>4</sub>-graphene hybrid (NCS-1/GNS), (c) tremella-like NCS-2, and (d) porous bead-cum needlelike NCS-3 and prepared by the MW-HT/ST method. The inset figures show the magnified FE-SEM images of the respective samples. (e) A comparative plot of J-V curves of DSSCs fabricated with different morphologies of pristine NiCo<sub>2</sub>S<sub>4</sub>, the NCS-1/GNS hybrid, Pt and pristine GNS counter-electrodes and a comparative histogram of power conversion efficiencies (PCEs) versus respective counter-electrodes (CEs). (f) Comparative IPCE spectra of DSSCs fabricated with different morphologies of pristine NiCo<sub>2</sub>S<sub>4</sub>, NCS-1/GNS hybrid, Pt and pristine GNS counter-electrodes showing high photoresponse. *Reproduced with permission from Royal Society of Chemistry R. Krishnapriya, S. Praneetha, A.M. Rabel, A. Vadivel Murugan, Energy efficient, one-step microwave-solvothermal synthesis of a highly electrocatalytic thiospinel NiCo<sub>2</sub>S<sub>4</sub>/graphene nanohybrid as a novel sustainable counter electrode material for Pt-free dye-sensitized solar cells, J. Mater. Chem. C 5 (12) (2017) 3146–3155.*



## 4.4 Conclusion

Energy conversion devices require efficient materials which possess distinctive electrical, optical, mechanical, and thermal properties. Recently, the development of nanoscience and technology has helped to meet the requirement of many materials for full application impact. During the past few years many multifunctional nanomaterials have been developed for energy applications. The advancement in this area is achieved by the properties such as excellent electrical and thermal conductivity, exceptionally large surface area, and chemical stability. The main challenges behind the multifunctional material are the higher performance limit, fewer functions, toxicity, availability, and high cost. Deep understanding of structure–property–relationship with the help of advanced characterization techniques is required in order to realize the large-scale commercial application of these materials. Although the energy conversion device performance using these materials enhanced considerably, to meet the future energy demands more developments are needed.

## Acknowledgments

Authors acknowledge financial support from PAN-IIT DBT center for Bioenergy grant number BT/EB/PANIIT/2012, Indian Institute of Technology Jodhpur for facilities and infrastructure support. We also acknowledge Dr. Kiran P Shejale for his contribution on research on DSSC.

## References

- [1] T.R. Cook, D.K. Dogutan, S.Y. Reece, Y. Surendranath, T.S. Teets, D.G. Nocera, Solar energy supply and storage for the legacy and nonlegacy worlds, *Chem. Rev.* 110 (11) (2010) 6474–6502.
- [2] P.V. Kamat, Meeting the clean energy demand: nanostructure architectures for solar energy conversion, *J. Phys. Chem. C* 111 (7) (2007) 2834–2860.
- [3] H. Wei, D. Cui, J. Ma, L. Chu, X. Zhao, H. Song, H. Liu, T. Liu, N. Wang, Z. Guo, Energy conversion technologies towards self-powered electrochemical energy storage systems: the state of the art and perspectives, *J. Mater. Chem.* 5 (5) (2017) 1873–1894.
- [4] J. Nowotny, J. Dodson, S. Fiechter, T.M. Gür, B. Kennedy, W. Macyk, T. Bak, W. Sigmund, M. Yamawaki, K.A. Rahman, Towards global sustainability: education on environmentally clean energy technologies, *Renew. Sustain. Energy Rev.* 81 (2018) 2541–2551.
- [5] M. Grätzel, Solar energy conversion by dye-sensitized photovoltaic cells, *Inorg. Chem.* 44 (20) (2005) 6841–6851.
- [6] Z.P. Cano, D. Banham, S. Ye, A. Hintennach, J. Lu, M. Fowler, Z. Chen, Batteries and fuel cells for emerging electric vehicle markets, *Nat. Energy* 3 (4) (2018) 279–289.
- [7] X. Tian, X.F. Lu, B.Y. Xia, X.W. Lou, Advanced electrocatalysts for the oxygen reduction reaction in energy conversion technologies, *Joule* 4 (1) (2020) 45–68.

- [8] H. Zhang, Y. Lu, W. Han, J. Zhu, Y. Zhang, W. Huang, Solar energy conversion and utilization: towards the emerging photo-electrochemical devices based on perovskite photovoltaics, *Chem. Eng. J.* 393 (2020) 124766.
- [9] X. Zhang, X. Cheng, Q. Zhang, Nanostructured energy materials for electrochemical energy conversion and storage: a review, *J. Energy Chem.* 25 (6) (2016) 967–984.
- [10] Q. Zhang, E. Uchaker, S.L. Candelaria, G. Cao, Nanomaterials for energy conversion and storage, *Chem. Soc. Rev.* 42 (7) (2013) 3127–3171.
- [11] M. Ye, M. Wang, Z. Lin, 1 - introduction: multifunctional photocatalytic materials: a perspective, in: Z. Lin, M. Ye, M. Wang (Eds.), *Multifunctional Photocatalytic Materials for Energy*, Woodhead Publishing, 2018, pp. 1–4.
- [12] Key attributes of nanoscale materials and special functionalities emerging from them, in *Nanoscale Multifunctional Materials* n.d., pp 1–32.
- [13] W.A. Badawy, A review on solar cells from Si-single crystals to porous materials and quantum dots, *J. Adv. Res.* 6 (2) (2015) 123–132.
- [14] J. Yan, B.R. Saunders, Third-generation solar cells: a review and comparison of polymer:fullerene, hybrid polymer and perovskite solar cells, *RSC Adv.* 4 (82) (2014) 43286–43314.
- [15] A. Sahu, A. Garg, A. Dixit, A review on quantum dot sensitized solar cells: past, present and future towards carrier multiplication with a possibility for higher efficiency, *Sol. Energy* 203 (2020) 210–239.
- [16] M.K. Assadi, S. Bakhoda, R. Saidur, H. Hanaei, Recent progress in perovskite solar cells, *Renew. Sustain. Energy Rev.* 81 (2018) 2812–2822.
- [17] H.S. Jung, J.-K. Lee, Dye sensitized solar cells for economically viable photovoltaic systems, *J. Phys. Chem. Lett.* 4 (10) (2013) 1682–1693.
- [18] F. Giustino, H.J. Snaith, Toward lead-free perovskite solar cells, *ACS Energy Lett.* 1 (6) (2016) 1233–1240.
- [19] Z. Ren, J. Wang, Z. Pan, K. Zhao, H. Zhang, Y. Li, Y. Zhao, I. Mora-Sero, J. Bisquert, X. Zhong, Amorphous TiO<sub>2</sub> buffer layer boosts efficiency of quantum dot sensitized solar cells to over 9%, *Chem. Mater.* 27 (24) (2015) 8398–8405.
- [20] P.V. Kamat, Quantum dot solar cells. Semiconductor nanocrystals as light harvesters, *J. Phys. Chem. C* 112 (48) (2008) 18737–18753.
- [21] G. Hodes, Comparison of dye- and semiconductor-sensitized porous nanocrystalline liquid junction solar cells, *J. Phys. Chem. C* 112 (46) (2008) 17778–17787.
- [22] X. Xia, J.H. Pan, X. Pan, L. Hu, J. Yao, Y. Ding, D. Wang, J. Ye, S. Dai, Photochemical conversion and storage of solar energy, *ACS Energy Lett.* 4 (2) (2019) 405–410.
- [23] M.C. Williams, Chapter 2 - fuel cells, in: D. Shekhawat, J.J. Spivey, D.A. Berry (Eds.), *Fuel Cells: Technologies for Fuel Processing*, Elsevier, Amsterdam, 2011, pp. 11–27.
- [24] S. Mekhilef, R. Saidur, A. Safari, Comparative study of different fuel cell technologies, *Renew. Sustain. Energy Rev.* 16 (1) (2012) 981–989.
- [25] A. Kirubakaran, S. Jain, R.K. Nema, A review on fuel cell technologies and power electronic interface, *Renew. Sustain. Energy Rev.* 13 (9) (2009) 2430–2440.
- [26] J.N. Tiwari, R.N. Tiwari, G. Singh, K.S. Kim, Recent progress in the development of anode and cathode catalysts for direct methanol fuel cells, *Nanomater. Energy* 2 (5) (2013) 553–578.
- [27] Chapter 41 - engineered nanomaterials for energy applications, in: C. Mustansar Husain (Ed.), *Handbook of Nanomaterials for Industrial Applications*, Elsevier, 2018, pp. 751–767.
- [28] M. Muthukumar, N. Rengarajan, B. Velliyangiri, M.A. Omprakas, C.B. Rohit, U. Kartheek Raja, The development of fuel cell electric vehicles – a review, *Mater. Today Proc.* (2020), <https://doi.org/10.1016/j.matpr.2020.03.679>.

- [29] M.-R. Gao, Y.-F. Xu, J. Jiang, S.-H. Yu, Nanostructured metal chalcogenides: synthesis, modification, and applications in energy conversion and storage devices, *Chem. Soc. Rev.* 42 (7) (2013) 2986–3017.
- [30] R.M. Ormerod, Solid oxide fuel cells, *Chem. Soc. Rev.* 32 (1) (2003) 17–28.
- [31] M. Grätzel, Dye-sensitized solar cells, *J. Photochem. Photobiol. C Photochem. Rev.* 4 (2) (2003) 145–153.
- [32] Q. Zhang, G. Cao, Nanostructured photoelectrodes for dye-sensitized solar cells, *Nano Today* 6 (1) (2011) 91–109.
- [33] M.A.M. Al-Alwani, A.B. Mohamad, N.A. Ludin, A.A.H. Kadhun, K. Sopian, Dye-sensitized solar cells: development, structure, operation principles, electron kinetics, characterisation, synthesis materials and natural photosensitisers, *Renew. Sustain. Energy Rev.* 65 (2016) 183–213.
- [34] Y. Qiao, C.M. Li, Nanostructured catalysts in fuel cells, *J. Mater. Chem.* 21 (12) (2011) 4027–4036.
- [35] T. Miyasaka, Toward printable sensitized mesoscopic solar cells: light-harvesting management with thin TiO<sub>2</sub> films, *J. Phys. Chem. Lett.* 2 (3) (2011) 262–269.
- [36] E.L. Ratcliff, B. Zacher, N.R. Armstrong, Selective interlayers and contacts in organic photovoltaic cells, *J. Phys. Chem. Lett.* 2 (11) (2011) 1337–1350.
- [37] R. Krishnapriya, S. Praneetha, A. Vadivel Murugan, Microwave-solvothermal synthesis of various TiO<sub>2</sub> nano-morphologies with enhanced efficiency by incorporating Ni nanoparticles in an electrolyte for dye-sensitized solar cells, *Inorg. Chem. Front.* 4 (10) (2017) 1665–1678.
- [38] H.-Y. Chen, D.-B. Kuang, C.-Y. Su, Hierarchically micro/nanostructured photoanode materials for dye-sensitized solar cells, *J. Mater. Chem.* 22 (31) (2012) 15475–15489.
- [39] F. Sauvage, F. Di Fonzo, A. Li Bassi, C.S. Casari, V. Russo, G. Divitini, C. Ducati, C.E. Bottani, P. Comte, M. Graetzel, Hierarchical TiO<sub>2</sub> photoanode for dye-sensitized solar cells, *Nano Lett.* 10 (7) (2010) 2562–2567.
- [40] X.-D. Qiao, Y.-Y. Liu, G.-L. Huang, B.-X. Lei, W. Sun, Z.-F. Sun, A multifunctional photoanode made of titania submicrospheres and titania nanoparticles modified titania nanotube arrays on FTO glass for dye-sensitized solar cells, *Mater. Sci. Semicond. Process.* 57 (2017) 99–104.
- [41] M. Adachi, Y. Murata, J. Takao, J. Jiu, M. Sakamoto, F. Wang, Highly efficient dye-sensitized solar cells with a titania thin-film electrode composed of a network structure of single-crystal-like TiO<sub>2</sub> nanowires made by the “oriented attachment” mechanism, *J. Am. Chem. Soc.* 126 (45) (2004) 14943–14949.
- [42] Z. Liu, M. Misra, Dye-sensitized photovoltaic wires using highly ordered TiO<sub>2</sub> nanotube arrays, *ACS Nano* 4 (4) (2010) 2196–2200.
- [43] Z. Hu, J.M. García-Martín, Y. Li, L. Billot, B. Sun, F. Fresno, A. García-Martín, M.U. González, L. Aigouy, Z. Chen, TiO<sub>2</sub> nanocolumn arrays for more efficient and stable perovskite solar cells, *ACS Appl. Mater. Interfaces* 12 (5) (2020) 5979–5989.
- [44] R. Krishnapriya, S. Praneetha, A. Vadivel Murugan, Energy-efficient, microwave-assisted hydro/solvothermal synthesis of hierarchical flowers and rice grain-like ZnO nanocrystals as photoanodes for high performance dye-sensitized solar cells, *CrystEngComm* 17 (43) (2015) 8353–8367.
- [45] K.P. Shejale, D. Laishram, M.S. Roy, M. Kumar, R.K. Sharma, On the study of phase and dimensionally controlled titania nanostructures synthesis at sub-zero temperatures, *Mater. Des.* 92 (2016) 535–540.
- [46] K.P. Shejale, D. Laishram, R.K. Sharma, High-performance dye-sensitized solar cell using dimensionally controlled titania synthesized at sub-zero temperatures, *RSC Adv.* 6 (28) (2016) 23459–23466.

- [47] K.P. Shejale, D. Laishram, R. Gupta, R.K. Sharma, Inside cover: zinc oxide–titania heterojunction-based solid nanospheres as photoanodes for electron-trapping in dye-sensitized solar cells (energy technol. 3/2017), *Energy Technol.* 5 (3) (2017), 355–355.
- [48] R. Krishnapriya, S. Praneetha, A.V. Murugan, Investigation of the effect of reaction parameters on the microwave-assisted hydrothermal synthesis of hierarchical jasmine-flower-like ZnO nanostructures for dye-sensitized solar cells, *New J. Chem.* 40 (6) (2016) 5080–5089.
- [49] R. Krishnapriya, S. Praneetha, S. Kannan, A. Vadivel Murugan, Unveiling the Co<sup>2+</sup> ion doping-induced hierarchical shape evolution of ZnO: in correlation with magnetic and photovoltaic performance, *ACS Sustain. Chem. Eng.* 5 (11) (2017) 9981–9992.
- [50] J. Song, L. Liu, X.-F. Wang, G. Chen, W. Tian, T. Miyasaka, Highly efficient and stable low-temperature processed ZnO solar cells with triple cation perovskite absorber, *J. Mater. Chem.* 5 (26) (2017) 13439–13447.
- [51] X. Dong, D. Chen, J. Zhou, Y.-Z. Zheng, X. Tao, High crystallization of a multiple cation perovskite absorber for low-temperature stable ZnO solar cells with high-efficiency of over 20%, *Nanoscale* 10 (15) (2018) 7218–7227.
- [52] Y. Wang, C. Ma, C. Wang, P. Cheng, L. Xu, L. Lv, H. Zhang, Design of SnO<sub>2</sub>@Air@TiO<sub>2</sub> hierarchical urchin-like double-hollow nanospheres for high performance dye-sensitized solar cells, *Sol. Energy* 189 (2019) 412–420.
- [53] R. Sasikumar, T.-W. Chen, S.-M. Chen, S.-P. Rwei, S.K. Ramaraj, Developing the photovoltaic performance of dye-sensitized solar cells (DSSCs) using a SnO<sub>2</sub>-doped graphene oxide hybrid nanocomposite as a photo-anode, *Opt. Mater.* 79 (2018) 345–352.
- [54] M. Park, J.-Y. Kim, H.J. Son, C.-H. Lee, S.S. Jang, M.J. Ko, Low-temperature solution-processed Li-doped SnO<sub>2</sub> as an effective electron transporting layer for high-performance flexible and wearable perovskite solar cells, *Nanomater. Energy* 26 (2016) 208–215.
- [55] P.C. Reshmi Varma, Chapter 7 - low-dimensional perovskites, in: S. Thomas, A. Thankappan (Eds.), *Perovskite Photovoltaics*, Academic Press, 2018, pp. 197–229.
- [56] C. Ma, N.-G. Park, A realistic methodology for 30% efficient perovskite solar cells, *Inside Chem.* 6 (2020) 1254–1264.
- [57] Z. Wang, Z. Shi, T. Li, Y. Chen, W. Huang, Stability of perovskite solar cells: a prospective on the substitution of the A Cation and X Anion, *Angew. Chem. Int. Ed.* 56 (5) (2017) 1190–1212.
- [58] D.P. McMeekin, G. Sadoughi, W. Rehman, G.E. Eperon, M. Saliba, M.T. Hörlantner, A. Haghighirad, N. Sakai, L. Korte, B. Rech, M.B. Johnston, L.M. Herz, H.J. Snaith, A mixed-cation lead mixed-halide perovskite absorber for tandem solar cells, *Science* 351 (6269) (2016) 151.
- [59] J. Huang, M. Lai, J. Lin, P. Yang, Rich chemistry in inorganic halide perovskite nanostructures, *Adv. Mater.* 30 (48) (2018) 1802856.
- [60] A.J. Jacobson, Materials for solid oxide fuel cells, *Chem. Mater.* 22 (3) (2010) 660–674.
- [61] S.P. Jiang, Development of lanthanum strontium manganite perovskite cathode materials of solid oxide fuel cells: a review, *J. Mater. Sci.* 43 (21) (2008) 6799–6833.
- [62] B.A. Boukamp, The amazing perovskite anode, *Nat. Mater.* 2 (5) (2003) 294–296.
- [63] Y. Zhang, M. Luo, Y. Yang, Y. Li, S. Guo, Advanced multifunctional electrocatalysts for energy conversion, *ACS Energy Lett.* 4 (7) (2019) 1672–1680.
- [64] Z. Yang, J. Ren, Z. Zhang, X. Chen, G. Guan, L. Qiu, Y. Zhang, H. Peng, Recent advancement of nanostructured carbon for energy applications, *Chem. Rev.* 115 (11) (2015) 5159–5223.

- [65] S.L. Candelaria, Y. Shao, W. Zhou, X. Li, J. Xiao, J.-G. Zhang, Y. Wang, J. Liu, J. Li, G. Cao, Nanostructured carbon for energy storage and conversion, *Nanomater. Energy* 1 (2) (2012) 195–220.
- [66] J.D. Roy-Mayhew, I.A. Aksay, Graphene materials and their use in dye-sensitized solar cells, *Chem. Rev.* 114 (12) (2014) 6323–6348.
- [67] J.-W. Lee, I. Jeon, H.-S. Lin, S. Seo, T.-H. Han, A. Anisimov, E.I. Kauppinen, Y. Matsuo, S. Maruyama, Y. Yang, Vapor-assisted ex-situ doping of carbon nanotube toward efficient and stable perovskite solar cells, *Nano Lett.* 19 (4) (2019) 2223–2230.
- [68] Y. He, S. Hwang, D.A. Cullen, M.A. Uddin, L. Langhorst, B. Li, S. Karakalos, A.J. Kropf, E.C. Wegener, J. Sokolowski, M. Chen, D. Myers, D. Su, K.L. More, G. Wang, S. Litster, G. Wu, Highly active atomically dispersed CoN<sub>4</sub> fuel cell cathode catalysts derived from surfactant-assisted MOFs: carbon-shell confinement strategy, *Energy Environ. Sci.* 12 (1) (2019) 250–260.
- [69] J. Shui, M. Wang, F. Du, L. Dai, N-doped carbon nanomaterials are durable catalysts for oxygen reduction reaction in acidic fuel cells, *Sci. Adv.* 1 (1) (2015) e1400129.
- [70] D. Laishram, K.P. Shejale, R. Krishnapriya, R.K. Sharma, Nitrogen-enriched carbon nanobubbles and nanospheres for applications in energy harvesting, storage, and CO<sub>2</sub> sequestration, *ACS Appl. Nano Mater.* 3 (4) (2020) 3706–3716.
- [71] H. Behret, H. Binder, G. Sandstede, Electrocatalytic oxygen reduction with thiospinels and other sulphides of transition metals, *Electrochim. Acta* 20 (2) (1975) 111–117.
- [72] N. Alonso-Vante, H. Tributsch, O. Solorza-Feria, Kinetics studies of oxygen reduction in acid medium on novel semiconducting transition metal chalcogenides, *Electrochim. Acta* 40 (5) (1995) 567–576.
- [73] M. Wang, A.M. Anghel, B. Marsan, N.-L. Cevey Ha, N. Pootrakulchote, S.M. Zakeeruddin, M. Grätzel, CoS supersedes Pt as efficient electrocatalyst for triiodide reduction in dye-sensitized solar cells, *J. Am. Chem. Soc.* 131 (44) (2009) 15976–15977.
- [74] Y.-C. Wang, D.-Y. Wang, Y.-T. Jiang, H.-A. Chen, C.-C. Chen, K.-C. Ho, H.-L. Chou, C.-W. Chen, FeS<sub>2</sub> nanocrystal ink as a catalytic electrode for dye-sensitized solar cells, *Angew. Chem. Int. Ed.* 52 (26) (2013) 6694–6698.
- [75] F. Gong, H. Wang, X. Xu, G. Zhou, Z.-S. Wang, In situ growth of Co<sub>0.85</sub>Se and Ni<sub>0.85</sub>Se on conductive substrates as high-performance counter electrodes for dye-sensitized solar cells, *J. Am. Chem. Soc.* 134 (26) (2012) 10953–10958.
- [76] X. Zhang, M. Zhen, J. Bai, S. Jin, L. Liu, Efficient NiSe-Ni<sub>3</sub>Se<sub>2</sub>/graphene electrocatalyst in dye-sensitized solar cells: the role of hollow hybrid nanostructure, *ACS Appl. Mater. Interfaces* 8 (27) (2016) 17187–17193.
- [77] S.-H. Chang, M.-D. Lu, Y.-L. Tung, H.-Y. Tuan, Gram-scale synthesis of catalytic Co<sub>9</sub>S<sub>8</sub> nanocrystal ink as a cathode material for spray-deposited, large-area dye-sensitized solar cells, *ACS Nano* 7 (10) (2013) 9443–9451.
- [78] X. Chen, J. Ding, Y. Li, Y. Wu, G. Zhuang, C. Zhang, Z. Zhang, C. Zhu, P. Yang, Size-controllable synthesis of NiCoSe<sub>2</sub> microspheres as a counter electrode for dye-sensitized solar cells, *RSC Adv.* 8 (46) (2018) 26047–26055.
- [79] J. Yang, Y. Niu, J. Huang, L. Liu, X. Qian, N-doped C/CoSe<sub>2</sub>@Co-FeSe<sub>2</sub> yolk-shell nano polyhedron as superior counter electrode catalyst for high-efficiency Pt-free dye-sensitized solar cell, *Electrochim. Acta* 330 (2020) 135333.
- [80] D. Ouyang, J. Xiao, F. Ye, Z. Huang, H. Zhang, L. Zhu, J. Cheng, W.C.H. Choy, Strategic synthesis of ultrasmall NiCo<sub>2</sub>O<sub>4</sub> NPs as hole transport layer for highly efficient perovskite solar cells, *Adv. Energy Mater.* 8 (16) (2018) 1702722.

- [81] J.-Y. Lin, S.-W. Chou, Highly transparent NiCo<sub>2</sub>S<sub>4</sub> thin film as an effective catalyst toward triiodide reduction in dye-sensitized solar cells, *Electrochem. Commun.* 37 (2013) 11–14.
- [82] M. Zhang, J. Zai, J. Liu, M. Chen, Z. Wang, G. Li, X. Qian, L. Qian, X. Yu, A hierarchical CoFeS<sub>2</sub>/reduced graphene oxide composite for highly efficient counter electrodes in dye-sensitized solar cells, *Dalton Trans.* 46 (29) (2017) 9511–9516.
- [83] R. Krishnapriya, S. Praneetha, A.M. Rabel, A. Vadivel Murugan, Energy efficient, one-step microwave-solvothermal synthesis of a highly electro-catalytic thiospinel NiCo<sub>2</sub>S<sub>4</sub>/graphene nanohybrid as a novel sustainable counter electrode material for Pt-free dye-sensitized solar cells, *J. Mater. Chem. C* 5 (12) (2017) 3146–3155.